Volume 8, December 2019 ISSN 2542-2545

The HIMALAYAN PHYSICS

A peer-reviewed Journal of Physics

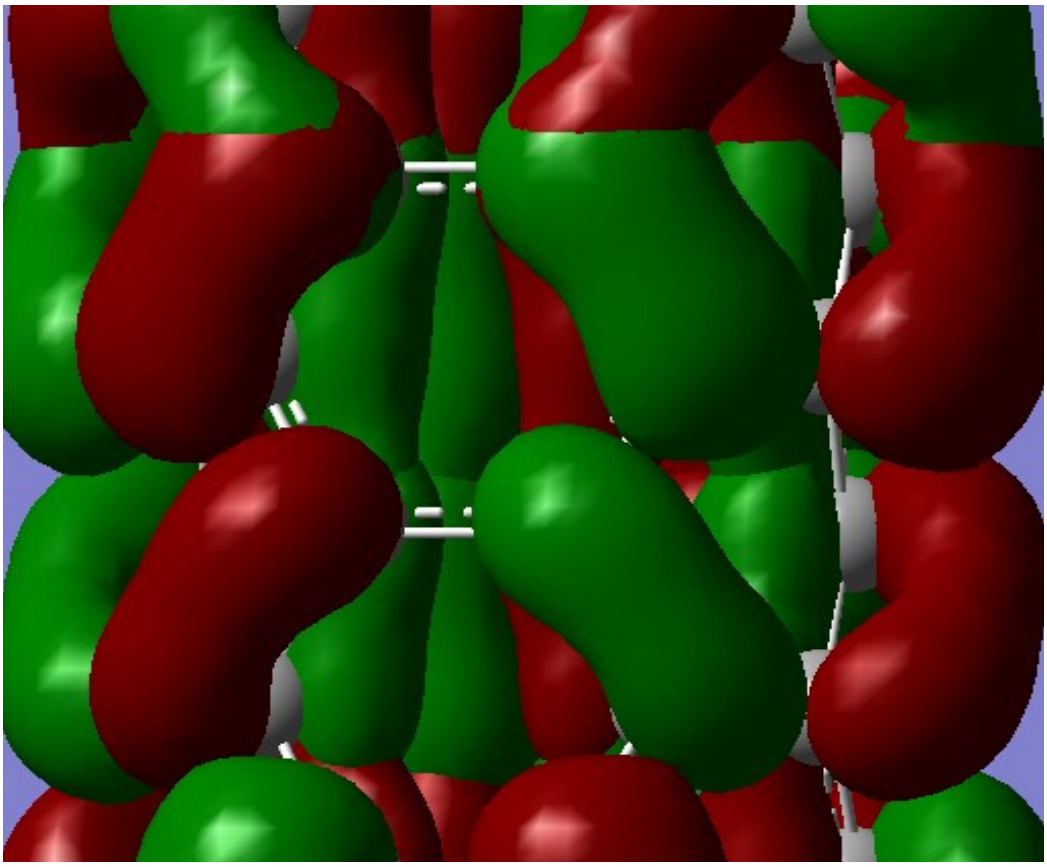

Department of Physics, Prithvi Narayan Campus, Pokhara
Nepal Physical Society, Western Chapter, Pokhara

Him. Phys. **8** 19-26, (2019)

Himalayan Physics

First principle study of chlorobenzene

Research Article

Devendra Singh Dhami, Bishoraj Joshi, Gagan Bahadur Dhami, Shantosh Bista, Bhawani Datt Joshi*

Department of Physics, Siddhanath Science Campus, Mahendranagar, 10406, Tribhuvan University, Nepal

Abstract: Chlorobenzene is a colourless flammable liquid used widely as a common solvent in the manufacture of other chemicals. In this communication, structural, electronic and vibrational study on chlorobenzene using Gaussian 09 program package employing B3LYP/6-31 G level of theory have been presented. The calculated IR and Raman spectra have been analyzed with the potential energy distribution. UV-Visible spectra taken in both the gaseous and solvent phase employing B3LYP/6-31G(d,p) level of theory have been given. The electronic transition between the frontiers energy levels together with their gap energy have analyzed.

Keywords: Chlorobenzene • IR • Raman • UV-Vis spectra

1. Introduction

Many aromatic compounds such as benzene derivative are commonly known for chronic inflammation treatment products in pharmaceutical field [1]. Chlorobenzene (Clbz) is a monocyclic aromatic compound with one hydrogen atom on the benzene ring substituted with one chlorine atom. It is a colorless flammable liquid with a sweet almond like odor, follow Huckel rule [2]. It has high solubility in non-polar solvents; however, it is almost insoluble in water.

It is common solvent and widely used intermediate in the manufacture of other chemicals. Clbz can persist in soil for several months, in air for about 3.5 days, and in water less than one day. When released to air it slowly breaks down by reactions with other chemicals and sunlight. In water, Clbz rapidly evaporates to the air or is broken down by bacteria [3]. The major use of Clbz is as an intermediate in the production of commodities such as herbicides, dyestuffs and rubber. It is also used as a high boiling solvent in many industrial applications as well as in the laboratory [4]. High level of Clbz can damage the liver and kidneys and affect the brain.

2. Computational Method

The geometrical parameter available from PubChem data base https://pubchem.ncbi.nlm.nih.gov/https://pubchem.ncbi.nlm.nih.gov/ has been used as the basis for the optimization. We optimized the ge-

* *Corresponding Author: pbdjoshi@gmail.com*

ometry, calculated the vibrational spectra by employing DFT/B3LYP/6-31G [5, 6] level of theory using Gaussian 09 program [7]. All the geometric parameters (bond length, bond angles and dihedral angles) have been obtained by the same level of theory. The different modes of vibrational frequencies together with their potential energy distributions have been analyzed. The electronic absorption wavelengths have been calculated both in the gaseous and the solvent (ethanol) phases by time dependent density functional theory (TD-DFT) [8]. Molecular electrostatic potential surface (MEP) has been mapped to know the molecular polarizability and its structure-activity relationship. UV-Visible spectra and MEP of the molecule was mapped. Vibration Frequencies were obtained from theoretical calculation and were scaled down by using wave number linear scaling procedure (WLS) [$\nu_{obs} = 1.0087 - 0.0000163\nu_{cal}$] [9]. The Infrared (IR) and Raman spectra were plotted using convoluted data by using origin pro software. All the calculations were performed at Siddhanath Science Campus, Mahendranagar, Nepal using a personal computer. The normal mode analysis was performed and the PED was calculated along the internal co-ordinates using localized symmetry. For this purpose, a complete set of 30 internal coordinates were defined using Pulay's recommendation [10, 11]. The 30 normal modes analysis was performed and the PED was calculated employing GAR2PED program [12] visualization and conformation of calculated data were done by using the CHEMCRAFT program [13].

3. Results and Discussion

Geometry Optimization

The ground sate optimized structure (in gas phase) of the molecule is as shown in the Fig. 1. The bond length between C-C of the molecules in HF/DFT was found to be 1.3949/ 1.3846 Å respectively. The bond length between C-H using HF was 1.0871 Å while in DFT it was 1.0714 Å. Also, the bond length between C-Cl in HF/DFT was 1.7213/1.8197Å, respectively and the bond angle between three carbon molecules was found to be 120.197° in DFT as well as 120.008° in HF. The calculated bond angle between C-C-H in DFT/HF was about to 121.154/ 120.809° respectively. The observed bond angle between C-C-Cl was found to be 118.821° in DFT and 120.004° in HF.

The thermal energy value of optimized molecule was 61.168 $kcal/mol$ and other thermodynamic parameters of optimized molecule like: specific heat capacity, entropy and zero point vibrational energy at room temperature were found to be 20.605 $kcal/mol, 76.204$ $kcal/mol$ and 57.746 $kcal/mol$, respectively in DFT calculation. The dipole moment was found to be 2.4324 Debye in gas phase and 2.8204 Debye in the solvent phase.

Molecular Electrostatic Potential

The net electrostatic effect, produced by the total charge distribution (electrons and nuclei) of a molecule at a point in space around it, is known as molecular electrostatic potential (MEP). The MEP provides visual method to understand the relative polarity of molecule which correlates the total charge distribution with dipole

moments, partial charges, electronegativity and site of chemical reactivity of a molecule. The different values of the electrostatic potential at the surface are represented by different colors. The red colour represents regions of most positive electrostatic potential, blue represents regions of most positive ESP and green represents regions of zero potential.

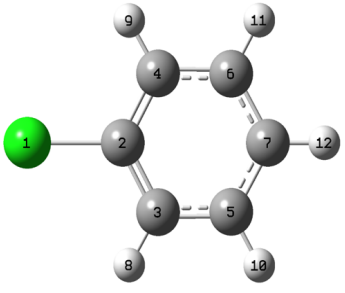

Figure 1. Optmized structure of Clbz.

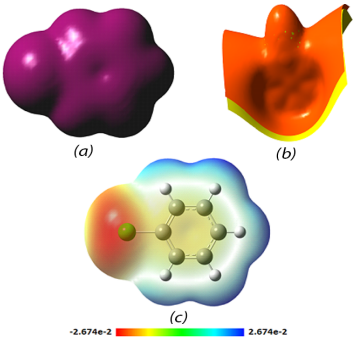

Figure 2. (a) Total density, (b) Electrostatic potential surface and (c) Molecular electrostatic potential.

Molecular electrostatic potential surface (MEP) of the molecule mapped with the output optimized by B3LYP/6-31G is as show in Fig. 2(c). The negative electrostatic potential (red regions) is localized over the chlorine atom that corresponds to an attraction of the proton by the aggregate electron density. The most positive regions (blue regions) correspond to proton repulsion (shaded as blue) are localized over hydrogen atoms. The electron density is uniform through whole the molecular vicinity (Fig. 2(a)). The yellowish blobs over chlorine atom reflect the negative ESP (Fig. 2(b)).

Electronic absorbance and HOMO-LUMO band gap

HOMO and LUMO play vital role in predicting electric and optical properties, higher the gap energy indicates more stability of molecules and vice-versa. Usually, a molecule with small frontier gap is more optically polarizable, kinetically less stable, has high conductivity and high reactivity in chemical reaction [14]. Fig. 3 shows UV-Vis spectrum of Clbz in gas and solvent phase. The electronic transition of high oscillatory strength(f) along with their absorption wavelength(λ) and excitation energies (E) and dipole moment(μ) for gas as well as solvent phase were obtained from DFT calculation employing 6-31G(d,p) level of theory [6] and listed in Table 1.

The first allowed transition H→L in gas phase was calculated as 228 nm with oscillator strength 0.0029 and in solvent phase it was at 230 nm (H→L) with oscillator strength 0.0021. The other main transitions in the gas phase were calculated at 205 nm (H→L+2), 200 nm (H→L+1), 177 nm (H–1→L+1), 175 nm (H–1→L), 155 nm (H–3→L) and 154 nm (H–3→L+1) with oscillator strengths 0.0015, 0.0661, 0.2590, 0.4495, 0.2822 and 0.1835, respectively. Similarly, in the solvent phase the main transition were at 214 nm (H→L+2), 204 nm (H→L+1), 180 nm (H–1→L), 180 nm (H–1→L+1), 156 nm (H–3→L) and 155 (H–3→L+1) with oscillator strengths 0.0008,

Table 1. Electronic transitions, absorption wavelength λ_{max} (nm), excitation energy (eV), oscillator strengths (f)

Excited State	Calculated								Transition type/ assignments
	Gas Phase				Solvent Phase(Ethanol)				
	λ_{max} (nm)	Transitions	$E(ev)$	Oscillator strength (f)	λ_{max} (nm)	Transitions	$E(ev)$	Oscillator strength (f)	
1	228	H→L	5.4283	0.0029	230	H→L	5.3818	0.0021	$\pi\rightarrow n*$
2	205	H→L+2	6.0484	0.0015	214	H→L+2	5.8060	0.0008	
3	200	H→L+1	6.1882	0.0661	204	H→L+1	6.0640	0.0648	
4	177	H-1→L+1	7.0025	0.2590	180	H-1→L	6.8759	0.6235	$\pi\rightarrow\pi^*$
5	175	H-1→L	7.0688	0.4495	180	H-1→L+1	6.8822	0.4165	
6	155	H-3→L	8.0156	0.2822	156	H-3→L	7.9711	0.1808	
7	154	H-3→L+1	8.0363	0.1835	155	H-3→L+1	7.9851	0.1103	$\pi\rightarrow\pi^*$

0.0648, 0.6235, 0.4165, 0.0022, 0.1808 and 0.1103, respectively. The calculated dipole moment in the solvent phase (2.8204) is higher than in gas phase (2.4324). The mainly transition which is observed in the UV-Vis spectrum is $\pi \rightarrow \pi^*$.

Similarly, the energy difference ($\Delta E = E_{LUMO}–E_{HOMO}$) between the two molecular orbital was -4.636 eV and -6.455 eV, respectively in the gas and solvent phases. Fig. 4 shows HOMO-LUMO plot for the different molecular orbitals taking part in the charge accumulation process in the gaseous phase. The red region indicates to positive charge and blue regions to the negative charge accumulating parts of the molecule. In figure clearly charge accumulated from HOMO to LUMO. In HOMO the charge is only accumulated from the ring as well as chlorine atom while in LUMO the charge accumulation is at C-H of the ring. In HOMO-1 the charge accumulation is at the ring carbon atom only, also in LUMO+1 the charge accumulation is at the carbon atom of ring.

Vibrational Assignment

Clbz, an aromatic compound, having 12 atoms is a nonlinear compound. So, it gives 30 (3N–6) normal modes of vibration. All the fundamental modes of vibration are both IR and Raman activities. The vibrational wavenumbers are obtained from the DFT calculation using Gaussian 09 program employing B3LYP/6-31G basis set. The calculated wavenumbers were scaled by wavenumber linear procedure (WLS) [$\nu_{obs} = 1.0087 - 0.0000163\nu_{cal}$] [9]. The calculated IR and Raman spectra with potential energy distribution are listed below in the Table 2. Further, the calculated IR and Raman spectra of the molecule are given in the Figs. 5 and 6 respectively. The vibrational assignments of the ring and functional groups have been given below:

C-H Vibration

There are five C-H and one C-Cl moieties in the title molecule as the functional groups. Generally, the C-H stretching modes are expected in the region 300-3000 cm^{-1} in the DFT [15, 16]. In this study, five C-H stretching modes were calculated in scaled DFT at 3096, 3093, 3081, 3069 and 3061 cm^{-1} with Raman activities 215.472, 9.785, 92.404, 97.443 and 42.395 a.u., and IR intensities 1.689, 2.078, 9.737, 7.822 and 0.047 (km/mol),

respectively. These pure modes were calculated in HF at 3106, 3103, 3090, 3079 and 3068 cm^{-1}, respectively.

The C-H in-plane deformation normally takes place as a number of strong to weak intensity sharp band in the region at 1300-1000 cm^{-1} in DFT [17–20]. The C-H in-plane deformation was calculated in scaled DFT at 1367 cm^{-1} with Raman activity 0.32 a.u. and IR intensity 0.565 a.u. This mode was calculated in HF at 1446 cm^{-1}.

The C-H out-of-plane deformation modes are expected in the region 1000-750 cm^{-1} in DFT [18, 19, 21, 22]. In the present study, the pure C-H out-of-plane deformation was calculated at 860/975 cm^{-1} in scaled DFT/HF. The mixed C-H out-of-plane deformations were calculated at 1032, 1004, 950 and 778 cm^{-1} in the DFT. Similarly, these wavenumbers were calculated at 1135, 1090, 1077 and 870 cm^{-1} in the HF.

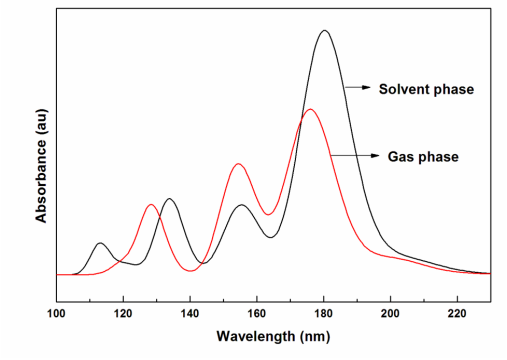

Figure 3. Theoretical UV-Visible spectra taken in gas phase (red) and solvent phase (black).

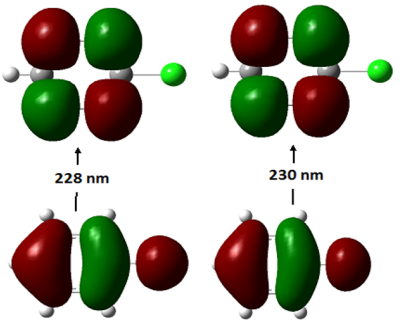

Figure 4. HOMO – LUMO plot of Clbz.

C-Cl vibration

In benzene ring, C-Cl bonds are formed in the place of hydrogen atoms. The C-Cl stretching band is normally expected around 750-580 cm^{-1} [23]. The calculated C-Cl stretching vibration mode by B3LYP method was at 402 cm^{-1} and assigned with Raman activities at 11.254 and IR intensities 8.11 a.u., respectively. This mode was observed in HF at 436 cm^{-1}. The C-Cl in-plane deformation was calculated at 277/ 311 cm^{-1} in the scaled DFT/HF, respectively. The C-Cl out-of-plane deformation was calculated at 487/545 cm^{-1} in DFT/HF as mixed mode.

Ring Vibration

In ring vibration C-C stretching, ring puckering, ring torsion, asymmetric deformation, asymmetric torsion and trigonal deformation are observed. Generally, the C-C stretching vibrations are expected in the region of 1430-1650 cm^{-1} [24]. In this study, C-C stretching vibrations were calculated at 1596, 1581, 1299, 1099, 1095 and 1026 cm^{-1} with Raman activities 12.495, 12.221, 0.469, 1.171, 7.003 and 36.086 a.u. and IR intensities 4.242, 23.853, 0.017, 3.666, 38.040 and 0.216 a.u., respectively in scaled DFT. The trigonal deformation of ring was calculated at 1054/1164 cm^{-1} in the DFT/HF with Raman activity 1.316 a.u. and IR intensity 24.151 a.u. The assigned value of scaled DFT for ring puckering was 726 cm^{-1} which is at 800 cm^{-1} in HF. The asymmetric ring

torsion vibrations were assigned at 653, 432 and 192 cm^{-1} in DFT. Similarly, these wavenumbers were calculated at 693, 545, 473 and 214 cm^{-1} in the HF.

Table 2. Calculated IR and Raman wavenumbers (using 6-31G level of theory).

Wavenumber			Raman	IR	Potential energy contribution (%)
Unscaled	Scaled				
DFT	DFT	HF			
3239	3096	3106	215.472	1.689	ν[CH](98)
3236	3093	3103	9.785	2.078	ν[CH](98)
3222	3081	3090	92.404	9.737	μ[CH](99)
3209	3069	3079	97.443	7.822	ν[CH](100)
3200	3061	3068	42.395	0.047	ν[CH](96)
1625	1596	1721	12.495	4.242	ν[CC](68) + δ_{in}[CH](20)
1609	1581	1715	12.221	23.853	ν[CC](64) + δ_{in}[CH](26)+R[δ_{as}](10)
1535	1510	1605	0.942	46.017	δ_{in}[CH](72) + ν[CC](30)
1505	1481	1568	0.221	7.946	δ_{in}[CH](66) + ν[CC](28)
1386	1367	1446	0.320	0.565	δ_{in}[CH](86)
1316	1299	1334	0.469	1.017	ν[CC](87) + δ_{in}[CH](12)
1235	1221	1289	4.386	0.002	δ_{in}[CH](72) + ν[CC](16)
1231	1217	1251	3.963	0.074	δ_{in}[CH](68) + ν[CC](20)
1109	1099	1171	1.171	3.666	ν[CC](60) + δ_{in}[CH](28)
1105	1095	1169	7.003	38.040	ν[CC](50) +ν[CC]19) + δ_{in}[CH](16) + R[δ_{tri}](11)
1064	1054	1164	1.316	24.151	R[δ_{tri}](73) + ν[CC](7)
1041	1032	1135	0.092	0.523	oop[CH](79) + R[puck](19)
1035	1026	1117	36.086	0.216	ν[CC](70) + R[δ_{tri}](20)
1012	1004	1090	0.080	0.000	oop[CH](90) + R[δ_{as}](9)
956	950	1077	1.298	5.167	oop[CH](87) + R[puck](6)
865	860	975	5.638	0.000	oop[CH](94)
781	778	870	2.455	49.402	oop[CH](63) +R[puck](36)
729	726	786	0.380	45.817	R[puck](64) + oop[CH](28)
711	709	755	5.947	29.379	R[δ_{as}](64) + ν[C2CL](25)
654	653	693	4.059	0.318	R[δ_{as}](89)
487	487	545	0.161	10.517	R[δ_{as}](55)+oop[CC](37)
431	432	473	0.004	0.000	R[δ_{as}](86) +oop[CH](14)
401	402	436	11.254	8.110	ν[CC](64)+R[δ_{as}](25)
275	277	311	2.078	0.328	δ_{in}[CC](90)
191	192	214	2.572	0.066	R[δ_{as}](44)+oop[CC](36)+oop[CH](14)

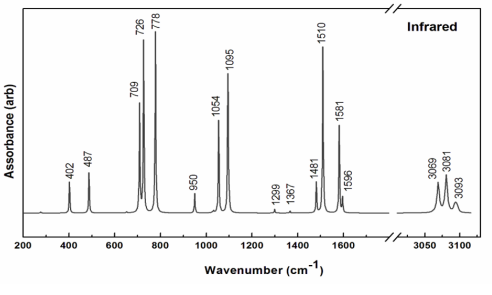

Figure 5. Calculated Infrared spectra of Clbz in the range 3150-200 cm^{-1}.

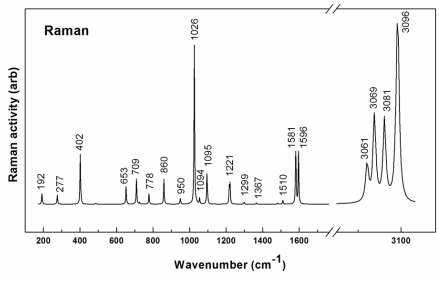

Figure 6. Calculated Raman spectra of Clbz in the range 3200-100 cm^{-1}.

4. Conclusions

Present study was mainly concentrated on the molecular structure, molecular electrostatic potential (ME), frontier energy level and vibrational frequency analysis of C6H5Cl (Clbz) using DFT. This molecule has 12 atoms and hence gives 30 modes of vibration. The equilibrium geometry and vibrational wavenumbers have been calculated using DFT and HF methods using Gaussian 09 program package employing 6-31 G basis set. All the calculated vibrational modes were found active both in IR and Raman. The MEP plot showed that the region near chlorine atom is most electronegative and the regions near hydrogen atoms are most electropositive. Further, the band gap (6.464 eV) between these two frontier energy levels show that the molecule is stable.

5. Acknowledgements

We are thankful to P. Tandon, Lucknow University, India for providing software facilities.

References

[1] Shakila G, Periandy S, Ramalingam S. Molecular structure and vibrational analysis of 1-bromo-2-chlorobenzene using ab initio HF and Density functional theory (B3LYP) calculations. Journal of Atomic, Molecular, and Optical Physics. 2011;2011:1–10.

[2] Jagdish S. Organic Chemistry Concepts and Applications. Pragati Prakashan; 2005.

[3] ATSDR. Toxicological profile for chlorobenzene. U.S. Public Health Service; 1990.

[4] Rossberg M, Lendle W, Pfleiderer G, Tögel A, Dreher EL, Langer E, et al. Ullmann's Encyclopedia of industrial chemistry-chlorinated hydrocarbons.; 2006.

[5] Hohenberg P, Kohn W. Inhomogeneous electron gas. Physical review. 1964;136(3B):B864–B871.

[6] Chong DP. Recent advances in density functional methods. vol. 1. Singapore: World Scientific; 1995.

[7] Frisch MJ, Trucks GW, Schlegel HB, Scuseria GE, Robb MA, Cheeseman JR, et al.. Gaussian˜09 Revision A.02; 2009. Gaussian Inc. Wallingford CT.

[8] Casida ME, Casida KC, Salahub DR. Excited-state potential energy curves from time-dependent density-functional theory: A cross section of formaldehyde's $^1A_1$ manifold. International journal of quantum chemistry. 1998;70(4-5):933–941.

[9] Yoshida H, Takeda K, Okamura J, Ehara A, Matsuura H. A new approach to vibrational analysis of large molecules by density functional theory: wavenumber-linear scaling method. The Journal of Physical Chemistry A. 2002;106(14):3580–3586.

[10] Pulay P, Fogarasi G, Pang F, Boggs JE. Systematic ab initio gradient calculation of molecular geometries, force constants, and dipole moment derivatives. Journal of the American Chemical Society.

1979;101(10):2550–2560.

[11] Fogarasi G, Zhou X, Taylor PW, Pulay P. The calculation of ab initio molecular geometries: efficient optimization by natural internal coordinates and empirical correction by offset forces. Journal of the American Chemical Society. 1992;114(21):8191–8201.

[12] Martin JML, Alsenoy CV. Gar2ped; 1995.

[13] Zhurko GA, Zhurko DA. Chemcraft;. Available from: www.chemcraftprog.com.

[14] Lewis D, Ioannides C, Parke D. Interaction of a series of nitriles with the alcohol-inducible isoform of P450: computer analysis of structure—activity relationships. Xenobiotica. 1994;24(5):401–408.

[15] Bellamy L. The infra-red spectra of complex molecules. 3rd ed. London: Chapman and Hall; 1975.

[16] George S. Infrared and Raman Characteristic Group Frequencies: Tables and Charts. 3rd ed. Wiley; 2004.

[17] Altun A, Gölcük K, Kumru M. Structure and vibrational spectra of p-methylaniline: Hartree-Fock, MP2 and density functional theory studies. Journal of Molecular Structure: THEOCHEM. 2003;637(1-3):155–169.

[18] Sundaraganesan N, Saleem H, Mohan S, Ramalingam M, Sethuraman V. FTIR, FT-Raman spectra and ab initio DFT vibrational analysis of 2-bromo-4-methyl-phenylamine. Spectrochimica Acta Part A: Molecular and Biomolecular Spectroscopy. 2005;62(1-3):740–751.

[19] Krishnakumar V, Prabavathi N. Simulation of IR and Raman spectral based on scaled DFT force fields: a case study of 2-amino 4-hydroxy 6-trifluoromethylpyrimidine, with emphasis on band assignment. Spectrochimica Acta Part A: Molecular and Biomolecular Spectroscopy. 2008;71(2):449–457.

[20] Joshi BD, Srivastava A, Tandon P, Jain S, Ayala A. A combined experimental (IR, Raman and UV–Vis) and quantum chemical study of canadine. Spectrochimica Acta Part A: Molecular and Biomolecular Spectroscopy. 2018;191:249–258.

[21] Krishnakumar V, Xavier RJ. Normal coordinate analysis of 2-mercapto and 4, 6-dihydroxy-2-mercapto pyrimidines. Indian Journal of pure and applied physics. 2003;41(8):597–601.

[22] Joshi BD. Structural, electronic and vibrational study of 4, 6-dichloro-5-methylpyrimidine: A DFT approach. Journal of Institute of Science and Technology. 2017;22(1):51–60.

[23] Hiremath C, Sundius T. Vibrational spectra, ab initio/DFT electronic structure calculations, and normal coordinate analysis of 2-bromo-5-fluorobenzaldehyde. Spectrochimica Acta Part A: Molecular and Biomolecular Spectroscopy. 2009;74(5):1260–1267.

[24] Sathyanarayana DN. Vibrational spectroscopy: theory and applications. New Age International; 2004.